

Operational shock response of ultrathin hard disk drives

Shengkai Yu¹ · Jianqiang Mou¹ · Wei Hua¹ · Weidong Zhou¹ · Chye Chin Tan¹

Received: 31 October 2014 / Accepted: 12 March 2015 / Published online: 22 March 2015
© Springer-Verlag Berlin Heidelberg 2015

Abstract Operational shock is one of the key challenges for designing ultrathin mobile hard disk drives (HDDs) due to the reduced thickness and stiffness of their mechanical components. The conventional operational shock simulations use the simplified models and methods that decouple the structural and air bearing dynamic analyses. These simplifications are not accurate as the coupling effect of air bearing and structural dynamics are ignored, and are even not valid in predicting the slider-disk contacts. In this paper, a method for the system level modelling and simulation of operational shock response of HDDs is proposed by integrating the structural finite element model of the HDD and the air bearing model, and coupling the structural dynamics analysis with the dynamic air bearing simulations. The dynamic shock response of the head-disk system in a 5 mm ultrathin HDD design is investigated. The effects of the drive base deformation together with the disk-ramp contact have been studied. The results reveal that the drive base deformation and disk-ramp contact are critical for the operational shock resistance performance of ultrathin drives.

1 Introduction

Ultrathin hard disk drives (HDDs) with a thickness of 5 mm or less are being developed for ultrathin, lightweight mobile computing devices and tablets by providing high capacity storage at an affordable price. Due to the applications in

highly mobile environment, and reduced thickness and stiffness of the mechanical components in ultrathin HDDs, the operational shock and vibration resistances is one of key performances in designing ultrathin HDDs. Specifically, the dynamic responses of the head disk system, and the head disk interface (HDI) under operational shock are crucial for the ultrathin HDDs to pass the industry standard reliability tests.

Early operational shock simulations by Zeng and Bogoy (2002) and Jayson et al. (2003) used the decoupled models where the air bearings were simplified as linear springs in finite element (FE) models to calculate the shock resistance loads under shock excitations first, and then these loads were applied to the slider in the air bearing code for dynamic air bearing simulations with the air bearing model. This decoupled method works well for the cases with the low level of shock excitations, as the air bearing stiffness can be considered linear, and there is no head-disk contact at such excitations. However, this method is not valid for the nonlinear cases, e.g. the statuses of slider lift-off or slider-disk contacts. Recently, a number of studies done by Jang and Seo (2007), Huang et al. (2013), and Mou et al. (2013) addressed on shock response and vibrations of HDDs by finite element analysis that focuses on the shock response of mechanical components of HDDs. The operational shock responses of HDI were also studied by simulations with considering the disk-ramp contacts by Rai and Bogoy (2011), and Li and Bogoy (2013). However, some mechanical components of HDDs are still ignored to simplify the problem. For example, the drive base deformation and spindle motor displacement are not considered in these simulations. But they actually play important roles to affect the disk-ramp contact, and therefore, the response of HDI.

In this paper, a method for system level modelling and simulation of operation shock responses of the air bearing slider, disk, ramp and drive base in the HDD is proposed by

✉ Shengkai Yu
yu_shengkai@dsi.a-star.edu.sg

¹ Data Storage Institute, Agency for Science, Technology and Research (A*STAR), DSI Building, 5 Engineering Drive 1, Singapore 117608, Singapore

coupling the air bearing model and the structural finite element model of the HDD that include its all major mechanical components. A code has been developed to integrate the structural dynamics analysis with the dynamic air bearing simulations. The dynamic shock responses of the head-disk system in a 5 mm thick ultrathin HDD design under an operational shock excitation with a typical 2 ms half sine pulse wave are studied by simulations with the developed models and methods. The drive base deformation, disk-ramp contact and displacements, and disk distortion have been included in the operational shock analysis, and their effects on the dynamic responses of the head-disk system are investigated.

2 System modeling and simulation method

The system model for operational shock simulations consists of two main parts: the reduced finite element model of the HDD structure, and the air bearing model. A coupled field fluid–structure dynamics simulation method is used to integrate these two parts of the models for operational shock simulations.

2.1 Structural finite element model

The commercial finite element software ANSYS is used to create the finite element model of the HDD. Figure 1

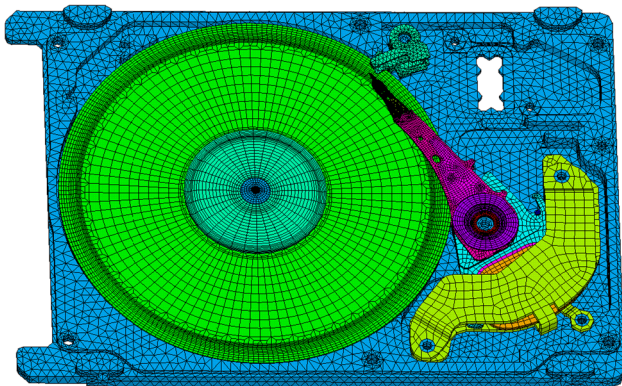
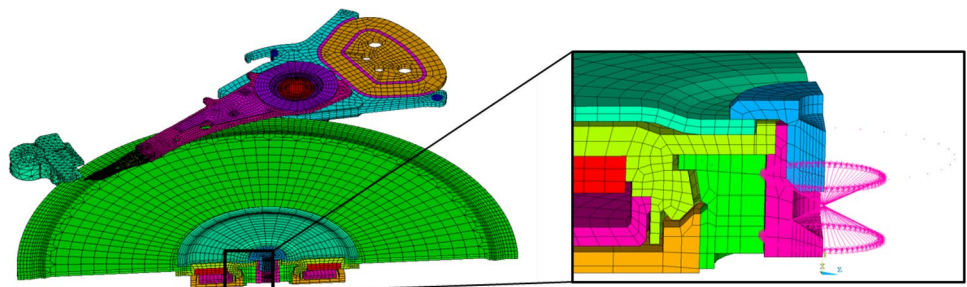


Fig. 1 Finite element model of the 5 mm ultrathin HDD

Fig. 2 FDB and pivot bearings in the ultrathin HDD



shows the full structural finite element model for a 5 mm thick ultrathin HDD design, where the meshed cover is hidden. This model includes all key mechanical components of the HDD, such as the base, spindle motor, disk, head suspension assembly (HSA), VCM actuator, pivot, ramp, and cover. In particular, the spring elements are used for modeling the fluid dynamic thrust bearing. The stiffness and damping matrices of fluid dynamic journal bearing of the motor spindle are modeled with two matrix27 elements, as displayed in Fig. 2. Furthermore, the matrix27 elements are used for modeling the radial and axial stiffness of the pivot bearings. Both of stiffness and damping parameters of the fluid dynamic bearings (FDB) and the pivot bearings are from the components supplier. The HSA including the suspension sag bend 2.2° and PSA 1.5° are assembled with the disk using a preload of 2.5 g, as shown in Fig. 3. The nodes at the 4 corners of the bottom slider's air bearing surface (ABS) are coupled with the adjacent nodes of the disk, respectively, while there is no constraint on the nodes of the top slider's ABS. The air bearing forces will be applied to the 4 corner nodes of the top slider's ABS during the coupled filed dynamic analysis.

The structure of the load-unload ramp is also included in the finite element model of the ultrathin HDD, as shown in Fig. 4. In this study, the disk-ramp contact is simplified as a point-to-point contact. So the spacing between the two adjacent nodes of the top ramp and the disk, and the two adjacent nodes of the bottom ramp and the disk will be used to decide whether the disk contacts with the ramp or they are separated. When the spacing is smaller than the minimal designed static clearance, a disk-ramp contact force is calculated based on the contact stiffness $K_c = 1e5$ N/m, and is then applied to the two nodes of the disk and the ramp, respectively. It is equivalent to the Lagrange multiplier method used by Li and Bogoy (2013).

It is good that the full HDD finite element model includes almost all mechanical components, however, it brings another big challenge: the high computational cost and low efficiency of the transient analysis due to the large scale of the finite element model. The number of the

degree-of-freedom (DOF) of the full HDD model is more than 600,000. It is impractical to use this large scale model for coupled-field dynamic analysis with the air bearing model. Actually it is also not necessary because this finite element model contains plenty of high frequency resonant modes which are not the real modes of the HDD structure. Here, a model order reduction (MOR) code is developed to reduce the scale of the model based on Krylov subspace methods reported by Salimbahrami and Lohmann (2006).

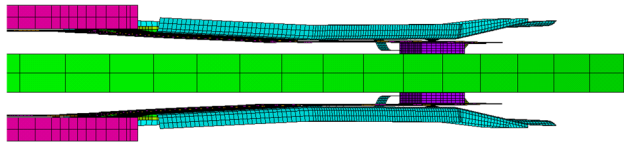


Fig. 3 Preloaded HSA assembled with disk

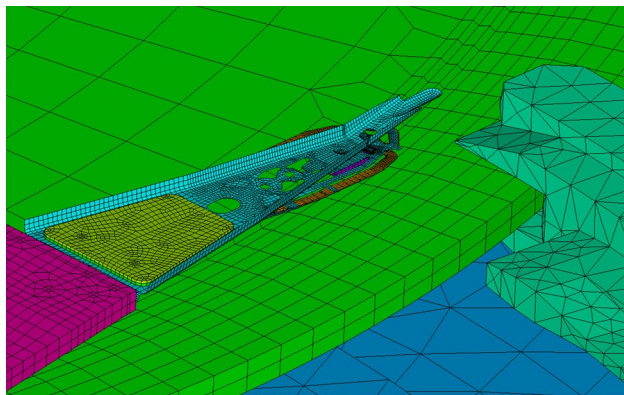


Fig. 4 Load-unload ramp, disk and head gimbal assembly

After the finite element model of the HDD is created, the mass, stiffness and damping matrices and force vectors of the HDD structural model can be extracted from ANSYS. Then the mass, stiffness and damping matrices and force vectors of the reduced model can be calculated with the MOR code. The reduced model consists of 667 DOFs only and includes the main resonant frequencies of the structure up to 200 kHz.

2.2 Air bearing model

The pressure distribution on the ABS is modeled using a generalized Reynolds equation as shown in Eq. (1).

$$\nabla(\tilde{Q}PH^3\nabla P - \tilde{\Lambda}PH) = \sigma_0\partial(PH)/\partial\tau \tag{1}$$

where P and H are the air bearing pressure and the slider/disk clearance, respectively; \tilde{Q} is the flow factor related to P and H ; $\tilde{\Lambda}$ is the bearing number; σ_0 is the squeeze number to represent the importance between the unsteady and diffusion effects; and τ is the time. The finite volume method is used for solving Eq. (1). The models of the air shear force and head-disk contact force described in the paper by Yu et al. (2006) and the intermolecular force model developed by Hua et al. (2007) are used in this study. A fast implicit algorithm by Hua et al. (2012) is employed for time-dependent dynamic simulations of air bearing sliders. Figure 5a shows the air bearing surface (ABS) of a ufemto slider (0.85, 0.7 and 0.18 mm) that is used in this study. The gram load is 24.5 mN. A static air bearing analysis is conducted. Figure 5b shows the air bearing pressure distribution on the ABS when the slider flies at the outer diameter location of the disk with a radius of 30.4 mm, a skew of 14.35°

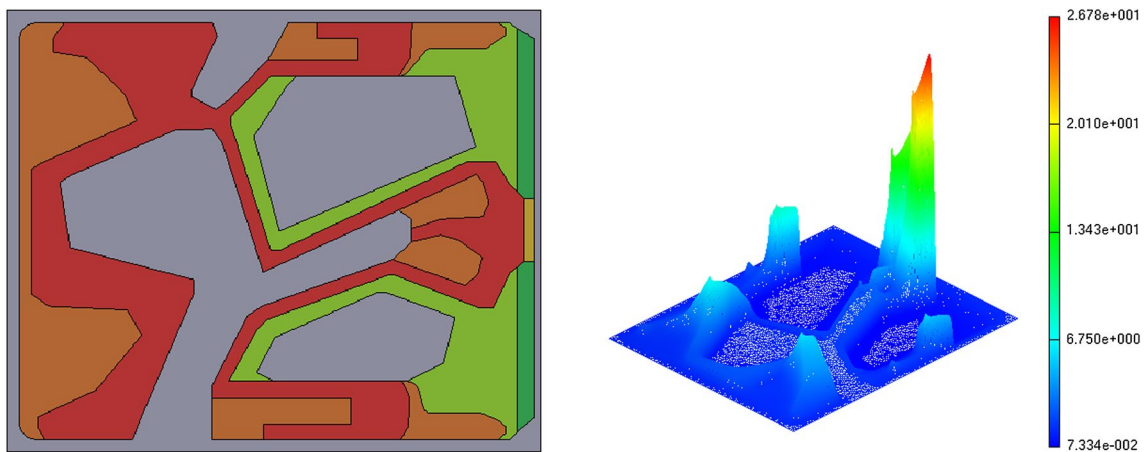


Fig. 5 a ABS design of an ufemto slider, b air bearing pressure distribution on the ABS

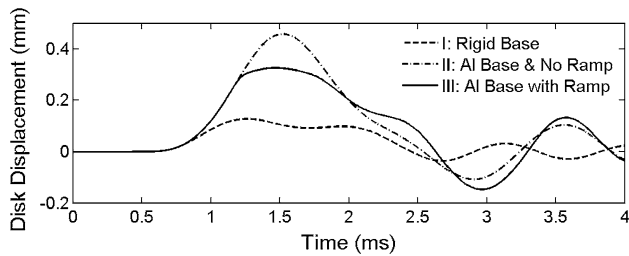


Fig. 6 Shock response of disk displacement at the outer diameter

and a spindle speed of 5400 rpm with the flying height of 11.2 nm, the pitch of 105 μrad , and the roll of $-3.5 \mu\text{rad}$.

2.3 Coupled-field analysis

To integrate the air bearing model with the finite element model of HDD mechanical components, a coupled-field fluid–structure simulation method is developed. The dynamic equation of motion can be written as:

$$[M]\{\ddot{u}\} + [C]\{\dot{u}\} + [K]\{u\} = \{F\} \quad (2)$$

where M , C and K are the mass, damping and stiffness matrices of the MOR model of the HDD, F is the sum of various forces on the MOR model, including the external excitation forces, the interface forces, such as the air bearing force obtained from Eq. (1), head-disk contact force, and intermolecular force at the interface, and other contact forces, such as the disk-ramp contact force. At each time step of the operational shock analysis, an iteration to calculate the slider's displacement related to the disk's displacement (or the slider's flying attitude) and the air bearing force is carried out till the predicted and the calculated slider's attitudes are converged. The disk-ramp contact will be monitored and considered at each time step. The procedure is repeated for the whole time duration to obtain the dynamic response of head-disk system. The details of the coupling analysis algorithm are described in the paper by Yu et al. (2006).

3 Results and discussions

3.1 Operational shock response of HDD components

Based on the simulation models and methods described above, a series of simulations have been done for a 5 mm thick ultrathin HDD with a disk rotation speed of 5400 rpm. A half sine shock pulse with a width of 2 ms starting from 0.5 ms and amplitude of 400G is applied to the drive which is fixed at the four screws of the drive. Three cases are studied: (1) the HDD with an assumed rigid base; (2) the HDD with the aluminum base but no ramp; and (3) the HDD with the aluminum base and the ramp.

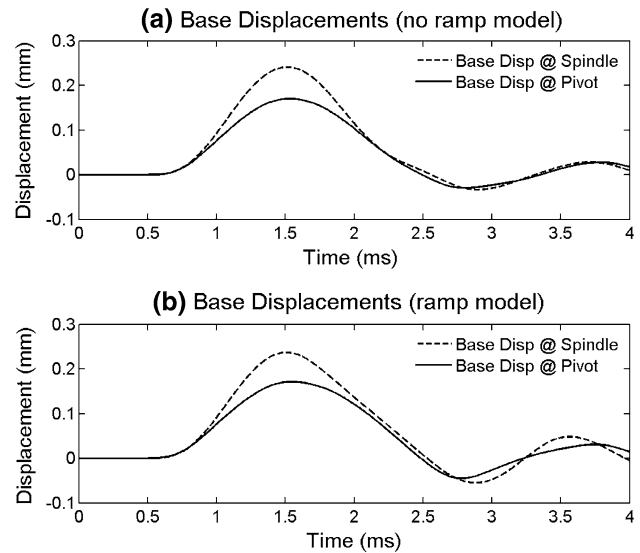


Fig. 7 Shock response of base displacements at positions of the spindle and the pivot for **a** no ramp model, and **b** ramp model

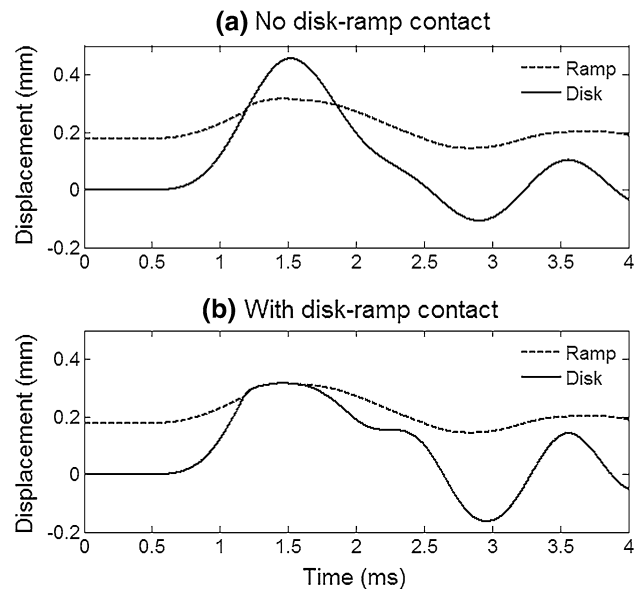
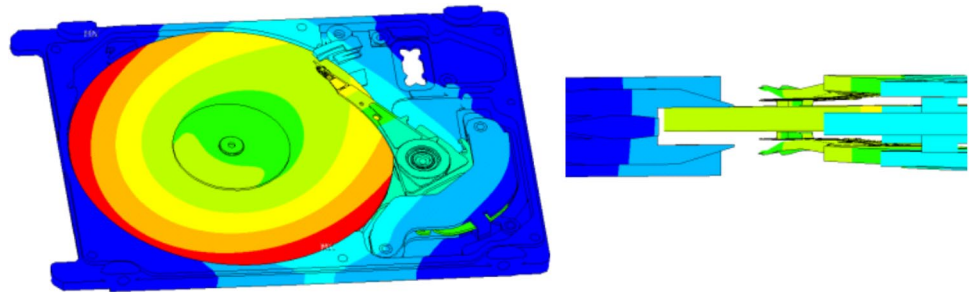


Fig. 8 The displacements of the ramp and the disk during the shock: **a** no disk-ramp contact, **b** with disk-ramp contact

The simulation results of the disk displacements at the location corresponding to the trailing edge center of the top slider are shown in Fig. 6. The results of the base displacements at the location of spindle center and pivot center are also plotted in Fig. 7. It is found that the maximum disk displacement in Case I (rigid base) is 127 μm only while it is 453 μm in Case II (aluminum base). This difference is caused by the base displacement. It indicates that the base displacement contributes to more than 70 % of the total disk displacement, due to the reduced stiffness (thickness)

Fig. 9 Displacement contour of HDD components during disk-ramp contact



of the base design in the ultrathin HDD. The relative displacement between the base locations of pivot and spindle may affect the shock responses of head-disk interface.

On the other hand, the amplitude of disk displacement is reduced by 30 % when the disk-ramp contact in the ultrathin HDD is included in the simulation. The disk-ramp contact also affects the base displacement at the spindle location, so as to change the relative displacement between the base locations at pivot and spindle, as shown in Fig. 7.

More importantly, the base deformation during the shock may significantly affect the disk-ramp contact. For HDD with rigid base model in Case I where the base deformation is not included, there is no disk ramp contact. The maximum disk displacement is 127 μm which is smaller than the disk ramp clearance (180 μm). However, when the base flexibility is considered and the disk ramp contact is ignored in the HDD model, i.e., Case II, the disk displacement is increased to 453 μm which far exceeds the disk ramp clearance, although the ramp node also has a small displacement due to the deformation of the ramp under the shock load, as shown in Fig. 8a. If the disk-ramp contact is considered, the ramp will restrict the displacement of the disk so that the disk and the ramp keep contacting, as shown in Fig. 8b. Figure 9 plots the displacement contour of HDD components during the disk-ramp contact. It is clearly seen that disk deformation is no longer the symmetric umbrella shape due to the disk-ramp contact.

3.2 Operational shock response of head-disk interface

The operational shock responses of the head-disk interface in Cases I, II and III are also compared. Figures 10–13 plot the simulation results of the top slider’s minimum clearance, air bearing force and slider-disk contact force, respectively, under the positive operational shock of half-sine 400G with a pulse width of 2 ms for the rigid base and no ramp model, the aluminum base and no ramp model, and the aluminum base with ramp model, respectively.

From the results of Case I shown in Figs. 10a and 12a, it can be seen that the slider has a larger displacement than the disk during the shock, so that the minimal clearance

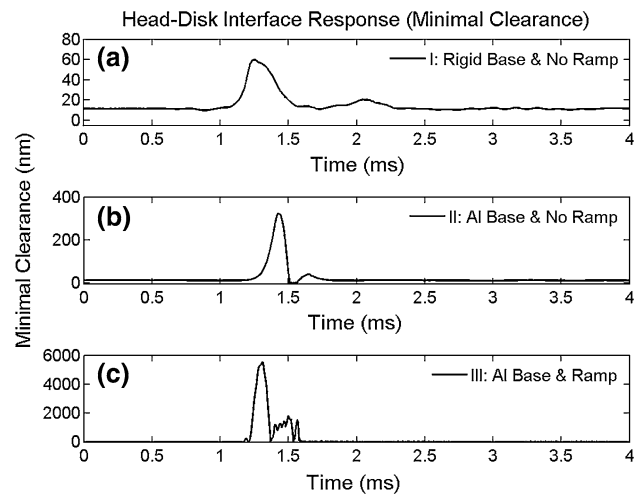


Fig. 10 Minimum clearance between the slider and disk under the operational shock for the model of **a** rigid base and no ramp (Case I), **b** Al base and no ramp (Case II), and **c** Al base and ramp (Case III), respectively

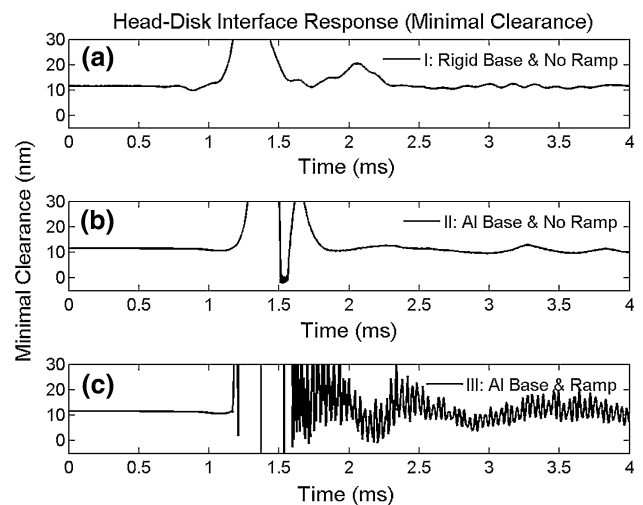


Fig. 11 Zoom-in view of minimum clearance between the slider and disk under the operational shock for the model of **a** rigid base and no ramp (Case I), **b** Al base and no ramp (Case II), and **c** Al base and ramp (Case III), respectively

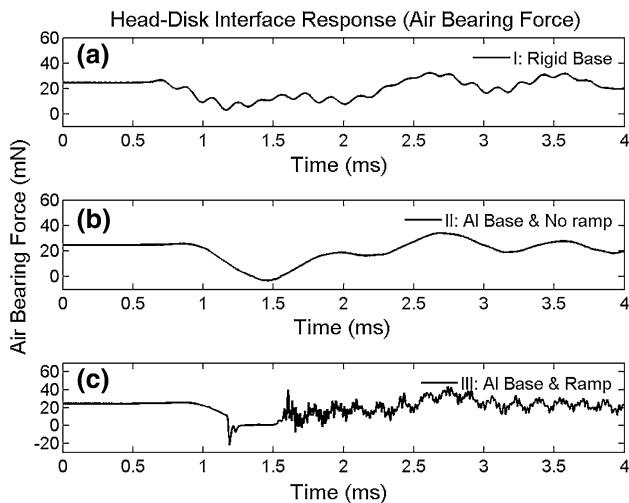


Fig. 12 Air bearing force between the slider and disk under the operational shock for the model of **a** rigid base and no ramp (Case I), **b** Al base and no ramp (Case II), and **c** Al base and ramp (Case III), respectively

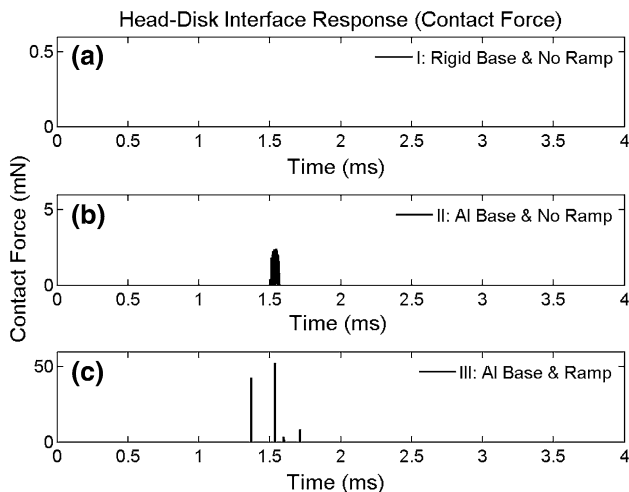


Fig. 13 Contact force between the slider and disk under the operational shock for the model of **a** rigid base and no ramp (Case I), **b** Al base and no ramp (Case II), and **c** Al base and ramp (Case III), respectively

between the slider and disk increases, the air bearing force decreases. It also can be seen that the clearance and air bearing force begins to oscillate slightly due to the vibrations of the suspension excited by the shock. But such spacing oscillations are not enough to lead to the head-disk contact, and the head-disk contact force keeps zero during the operational shock, as shown in Fig. 13a. From the results of Case II shown in Figs. 10b and 11b, it can be found that the minimal clearance between the slider and disk increases to more than 300 nm, and then drops to zero, which indicates head-disk contact. Some very low level of

head-disk contacts can be observed from Fig. 13b. But no large suspension vibrations are excited, as seen from the results of the clearance and air bearing force in Figs. 11b and 12b, respectively. From the results of Case III shown in Fig. 10c, it can be seen that the minimal clearance increases to almost 6000 nm that indicates slider is lifted off. A sudden clearance increase and a sudden air bearing force drop can be observed at 1.2 ms from the zoom-in view of the minimal clearance in Fig. 11c, and the air bearing force in Fig. 12c, respectively, which are caused by the disk-ramp contact. When the slider drops and is loaded, the big head-disk contacts can be observed in Fig. 13c, which excite the high frequencies of suspension/gimbal vibrations, as shown in Figs. 11c and 12c.

From the simulation results, it can be found that the drive base deformation and the disk-ramp contact play the critical role for the operational shock resistance performance of ultrathin HDDs. At the shock of 400G @ 2 ms, the rigid base model gives the smaller flying attitude response, and no head-disk contact occurs. When the deformation of the drive base is considered in the model of HDD with the aluminum base and no ramp, the flying attitude response is much larger, and minor head-disk contacts are observed. The total air bearing force profile looks different from the HDD with rigid base model. When the deformable base and ramp are included in the model, the slider lift-off and head-disk contacts occur. The results reveal that the disk-ramp contact will lead to the head-disk contact during the operational shock and degrade the operational shock resistance of the head-disk interface. The stiffer base will decrease the relative motion between the disk and the ramp, so as to reduce the disk-ramp contact force, and therefore, decrease the possibility of HDI failure and enhance the operational shock resistance performance of HDDs.

4 Conclusions

This paper studies the operational shock response of ultrathin HDDs, and the effects of reduced HDD component stiffness due to the reduction of their thickness. A method for system level modeling and simulation of operational shock responses of the HDD has been developed, by coupling the finite element model of the HDD structure and the air bearing model. A full structural finite element model for a 5 mm thick ultrathin HDD design is created, and the reduced model is obtained by the model order reduction so as to benefit from both including more parameters of mechanical components and achieving high computational efficiency. Operational shock simulation studies of the head-disk system for disk spinning at 5400 rpm in a 5 mm thick ultrathin HDD, under the half-sine 400G @ 2 ms operational shock pulse wave have been carried out.

The effects of drive base stiffness together with the disk-ramp contact have been investigated. It is concluded that base stiffness and disk-ramp contact have substantial influence on the operational shock responses of the ultrathin HDDs, and should not be ignored anymore. The stiff base design can effectively improve the 2 ms operational shock resistance performance of ultrathin HDDs. More parametric studies based on this model and method will be carried out in the future.

References

- ANSYS, ANSYS Inc., <http://www.ansys.com>
- Hua W, Liu B, Yu SK, Zhou WD (2007) Probability model for the intermolecular force with surface roughness considered. *Tribol Int* 40:1047–1055
- Hua W, Yu SK, Zhou WD, Myo KS (2012) A fast implicit algorithm for time-dependent dynamic simulations of air bearing sliders. *ASME J Tribol* 134:031901
- Huang L, Suzuki K, Huang FY, Hirano T, Stipe B (2013) “HAMR HDD shock responses”. In: *Proceedings of the ASME ISPS2013*, Santa Clara, California, ISPS2013–2896, 24–25 June 2013
- Jang GH, Seo CH (2007) Finite-element shock analysis of an operating hard disk drive considering the flexibility of a spinning disk-spindle, a head-suspension-actuator, and a supporting structure. *IEEE Trans Magn* 43(9):3738–3743
- Jayson EM, Smith PW, Talke FE (2003) Shock modelling of the head-media interface in an operational hard disk drive. *IEEE Trans Magn* 39(5):2429–2431
- Li L, Bogy DB (2013) Numerical analysis of head disk interface response during operational shock with disk-ramp contact. *IEEE Trans Magn* 50(4):1–6
- Mou JQ, Lai F, See IBL, Lin WZ (2013) Analysis of structurally transmitted vibration of HDD in notebook computer. *IEEE Trans Magn* 49(6):2818–2822
- Rai R, Bogy DB (2011) Parametric study of operational shock in mobile disk drives with disk-ramp contact. *IEEE Trans Magn* 47(7):1878–1881
- Salimbahrami B, Lohmann B (2006) Order reduction of large scale second-order systems using Krylov subspace methods. *Linear Algebra Appl* 415:385–405
- Yu SK, Liu B, Hua W, Zhou WD (2006) Contact-induced off-track vibrations of air bearing-slider-suspension system in hard disk. *Tribol Lett* 24(1):27–36
- Zeng QH, Bogy DB (2002) Numerical simulation of shock response of disk-suspension-slider air bearing systems in hard disk drives. *Microsyst Technol* 8:289–296